Journal of Mountain Area Research
Vol. 8, 2023
https://doi.org/10.53874/jmar.v8i0.175

Full length article

MHD STAGNATION POINT FLOW WITH THERMAL RADIATION AND SLIP EFFECT OVER A LINEAR STRETCHING SHEET

*Ubaidullah Yashkun[1,2,] *, Khairy Zaimi[1], Liaquat Ali Lund[3]*

1. Faculty of Applied Human and Sciences, Boundary Layer Research Group, Institute of Engineering Mathematics, Universiti Malaysia Perlis, Arau, Malaysia
2. Department of Mathematics and Social Sciences, Sukkur IBA University, Sukkur, Pakistan
3. School of Quantitative Sciences, Universiti Utara Malaysia, 06010 Sintok, Kedah, Malaysia

ABSTRACT

This research investigates the flow of stagnation point magnetohydrodynamic (MHD) and heat transfer along the stretched sheet in the existence of radiation and slip effects. With the help of similarity variables, the governing partial differential equations (PDEs) are transformed into ordinary differential equations (ODEs). The BVP4C technique in Matlab function has been used to simplify the governing ODEs. The numerical outcomes for temperature and velocity profiles, coefficient of skin friction and Nusselt Number have been achieved and matched with the findings in literature. The findings are compared to previously reported results. In addition, the impacts of numerous related parameters on the profiles of velocity and temperature are shown, and the results of every related parameter are presented using graphs. The velocity profile decreases as the magnetic force, suction, and permeability parameters rise.

Keywords: Thermal radiation; slip effect; magnetohydrodynamic (MHD); suction; Prandtl number

*Corresponding author: (ubaidullah@iba-suk.edu.pk)

1. INTRODUCTION

In scientific literature, an extensive body of research has been done using stagnation points over the stretching sheet. It is widely used in a variety of engineering and manufacturing area, including insulating materials, polymer sheet production, glass drawing, production, displacement, and continuous casting, it is well-known in the researchers. With the use of comparable variables, Hiemenz [1] claimed that equations of Navier–Stokes may be translated into 3rd order ODEs, which became known as two-dimensional stagnation point flow. Sakiadis [2] gave mathematical solutions for boundary layer flow on the stretched surface in his paper. The exponentially stretched surface and the linearly stretched surface were further developed by Crane [3] in 1970. Chiam [4] investigated the flow of a stagnation point towards a bending plate. Several researchers, including Ishak et al. [5], have studied the MHD flow of stagnation point approaching a vertical stretched surface. Sadeghy et al. [6] examined flow of stagnation point of Maxwell fluid in a two-dimensional. Attia [7] studied the viscous fluid flow affecting on a porous stretched sheet for heat absorption in three dimensions using hydromagnetic flow of laminar and stagnation point. Recently, Ghasemi and Hatami [8] explored the stagnation point of nanofluid flow in conjunction with the effects of solar radiation for MHD nanofluid flow.

As a result of recent advances in research, magnetohydrodynamics (MHD) may be thought of the mix of mechanics of fluids and electromagnetism, specifically the action of magnetic on an electrically conducting fluid, or both. Many studies have recently concentrated on the study of MHD flow because of its importance in a wide range in the field of Plasma Physics and engineering applications, including oil refinery, MHD power generators, the reactor of nuclear power, chemical reactions, magnetic mixers, and boundary layer control in aerodynamics [9-12]. Here, we will discuss several recent research that has concentrated on the MHD influence on heat transfer and flow concerns. These studies also focused on the flow and heat transfer of a viscous and incompressible fluid passing through a stretching surface along with magnetic field, among other fluids that are used in the industrial setting. According to Darzi et al. [13], for instance, they looked at the impact of heat transfer via the porous medium on the profile of velocity and temperature due to a thin liquid film flowing through a stretching sheet. Nandeppanavar et al. [14] used a porous stretched sheet and thermal radiation to investigate the MHD flow of stagnation point 2D via a porous medium. Abel and Nandeppanavar [15] investigated the impacts of non-uniform temperature sources and thermal radiation on MHD viscoelastic fluid movement and heat transmission past a stretched surface. Mustafa and Khan [16] explored the 2D steady next to the boundary, the mass transfer of Casson nano fluid, and the heat transmission of this liquid in existence of an exponential stretched surface. Khalili et al. [17] quantitatively examined heat transfer of MHD flow of three distinct nanofluids induced through the shrunk plane inside porosity medium. Ghasemi et al. [18] simulated the MHD blood flow through porous vessels using both analytical and numerical methods. They classified blood like a 3rd grade fluid comprising nanoparticles, according to their classification. Asadi et al. [19] study the natural CuO-TiO2/water hybrid nanofluid at two infinite parallel vertical plates that are infinitely parallel to one another. They discovered that as volume percentage of nanoscale particles improves, width of momentum boundary increases while width of thermal layer decreases.

Several practical applications relating to the boundary flow immerse in media of porous, including heat exchangers, geothermal engineering, oil industries, nuclear waste destruction, system of the grain storage, and others have drawn great interest to the research of boundary layer flow embedded in porous medium. Nield and Bejan [20] have highlighted the advantages of heat transfer flow across porous material and how it might be used. Several researchers, including Mohanty et al. [21], have studied approximate solutions for the transport of heat and mass of a micropolar fluid passing through porous media. Working on the MHD convective flow with reaction of chemical and radiation on porous medium [22]. Prasad et al. [23] explored the oscillatory reaction on viscoelastic fluid passing in porous media caused by a stretched sheet in a porous media. A study by Shamshuddin et al [24] investigated flow of MHD of the micropolar liquid using permeable medium over a moving surface that was incline. Many of the authors have recently completed simulations of porous medium interactions under a variety of flow conditions, which are detailed in the references [25-30].

This study expands the prior model of Agbaje et al. [31] to include the impact of MHD slip and radiation on heat transfer owing to flow of stagnation of nano-liquid across the stretching surface, which was previously neglected. Because of the linear similarity conversions, the conservation equalities are reduced to a dimensionless state. In order to simulate the nanofluid, an interfacial boundary condition is introduced, and an effective and reliable numerical approach, the BVP4C technique in Matlab function, according to the authors. Detailed research is conducted to determine how important parameters affect flow rate and energy output. The findings have been supported by results from prior investigations, which have been tabulated and found to have an excellent connection with the findings of the current study.

2. PROBLEM FORMULATION

In this study considered steady, MHD fluid flow in a porous form of boundary layer towards the stagnation point with effect of slip and thermal radiation long a stretched surface. The free stream velocity $U_{\infty}(x) = bx$ and the stretching velocity $U_w(x) = ax$ are along the flow direction. The constants a and b areas $a > 0$ and $b \geq 0$. The ambient temperature is T_{∞} and the mass flux velocity is $V_w(x)$. The flux velocity $V_w(x) = -(a\nu)^{1/2}S$. The surface temperature of the stretching sheet is $T_w(x) = T_{\infty} + cx^n$, where c and n are constant as $c > 0$ at the heated surface. The proposed model is demonstrated using the following set of PDEs [31]. The physical model is presented in Figure 1.

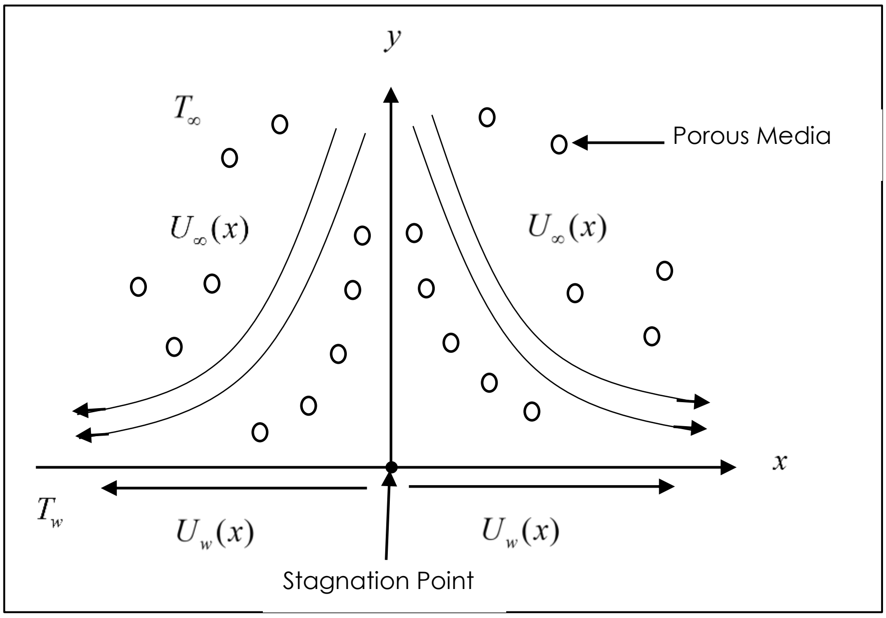

Figure 1. Geometry of Fluid Flow Model.

$$\frac{\partial u}{\partial x}+\frac{\partial v}{\partial y}=0, \tag{1}$$

$$u\frac{\partial u}{\partial x}+v\frac{\partial v}{\partial y}=U_\infty\frac{dU_\infty}{dx}+\nu\frac{\partial^2 u}{\partial y^2}+\sigma\frac{B_0^2}{\rho}(U_\infty-u)+\frac{\nu}{K}(U_\infty-u), \tag{2}$$

$$u\frac{\partial T}{\partial x}+v\frac{\partial T}{\partial y}=\alpha\frac{\partial^2 T}{\partial y^2}+\frac{Q}{\rho c_p}(T-T_\infty)-\frac{\alpha}{K}\frac{\partial q_r}{\partial y}, \tag{3}$$

with the boundary conditions

$$u=U_w(x)+L\left(\frac{\partial u}{\partial y}\right), v=V_w(x), T=T_w(x), \text{when } y=0$$
$$u\to U_\infty(x), T\to T_\infty \text{as} y\to\infty \tag{4}$$

In the system of equations (1)-(4) u,v are the velocity components along the axis of x,y respectively. The parameters are $\rho,\nu,K,\alpha,c_p,Q,L,\sigma$ and q_r the fluid density, kinematic viscosity, porous medium permeability, thermal diffusivity, specific heat capacity, heat source/sink ($Q>0, Q<0$), slip effect, electrical conductivity, and heat flux.

PDEs (2-3) are transformed into ODEs using similarity transformation.

$$f(\eta)=\frac{\psi}{(a\nu)^{\frac{1}{2}}x}, \theta(\eta)=\frac{T-T_\infty}{T_w-T_\infty}, \eta=\left(\frac{a}{\nu}\right)^{\frac{1}{2}}y, \tag{5}$$

ψ is the stream function and its definition is as follows:

$$u=\frac{\partial\psi}{\partial y} \text{ and } v=-\frac{\partial\psi}{\partial x} \tag{6}$$

The velocity components u and v became.

$$u=axf'(\eta), v=-(a\nu)^{\frac{1}{2}}f(\eta) \tag{7}$$

Where (′) represents differentiation w.r.t. η, γ is the suction/injection parameter where $\gamma>0$ shows suction effect and $\gamma<0$ indicates the injection effect. The transformed ODEs are as

$$f'''+ff''-f'^2+B^2+M(B-f')-(\Gamma-B)f', \tag{8}$$

$$\frac{1}{P_r}\left(1+\frac{4}{3}R\right)\theta''+A\theta+f\theta'-n\theta f' \tag{9}$$

The boundary conditions are as

$$f(0)=\gamma, f'(0)=1+\delta f''(0), \theta(0)=1,$$
$$f'(\infty)=B, \theta(\infty)=0 \tag{10}$$

Where $B=\frac{b}{a}$ is velocity ratio, $M=\frac{\sigma B_0^2}{a\rho}$ is magnetic, $\Gamma=\frac{\nu}{aK}$ is the permeability parameter, $A = \frac{Q}{a\rho c_p}$ is the dimensionless heat generation/absorption coefficient, $R = \frac{4\sigma^* T_\infty^3}{KK_s}$ is the thermal radiation and $\delta = (\frac{b}{v})^{1/2} L$ is the slip parameter.

The "substantial physical quantities of interest are the skin friction C_f and Nusselt number Nu_x are as

$$C_f = \frac{\tau_w}{\rho_f U_\infty^2}, Nu_x = \frac{x q_w}{K_f (T_w - T_\infty)}, \tag{11}$$

where τ_w is the shear stress along the plate's surface and q_w is the heat flow from the plate, the equations are as follows:

$$\tau_w = \mu(\frac{\partial u}{\partial y})_{y=0}, q_w = -K(\frac{\partial T}{\partial y})_{y=0} + (q_r)_{y=0}, \tag{12}$$

Putting Equation (5) into Equation (11) with (10), one can get

$$C_f\, Re_x^{\frac{1}{2}} = f''(0), \frac{Nu_x}{Re_x^{\frac{1}{2}}} = -\left(1 + \frac{4}{3}R\right)\theta'(0), \tag{13}$$

Where $Re_x = \frac{U_w(x)x}{\nu}$ is the Reynolds number.

3. NUMERICAL PROCEDURE AND VALIDATION

We used the Three Stage Labatto Three A Scheme in conjunction with the BVP4C technique to numerically solve the transformed ODEs (08-10) in order to find the solution. To make the problem simpler, all of the modified equations are expressed in the form of an initial value problem (IVP). In this case the initial values of $f''(0)$ and $\theta'(0)$ are not known. The BVP4C is used to determine the of $f''(0)$ and $\theta'(0)$ by picking a specific value of $\eta \to \infty$ and a few starting guesses. The procedure of forecasting initial guesses is repeated until the desired value of the iteration is achieved. To turn Equations (08-10) into the first order ODEs, we must take into account the following variables:

$$f = y_1, f' = y_2, f'' = y_3, \theta = y_4, \theta' = y_5 \tag{14}$$

$$f''' = y_2 * y_2 - y_1 * y_3 - B^2 - M * (B - y_2) + \Gamma y_2 \tag{15}$$

$$\theta'' = \left(\frac{3 * Pr}{3 + 4 * R}\right)\{n * y_4 * y_2 - A * y_4 - y_1 * y_5\} \tag{16}$$

Subject to boundary conditions

$$y_1(0) = \gamma, y_2(0) = 1 + \delta * \alpha_1, y_3(0) = \alpha_1 \quad y_4(0) = 1, y_5(0) = \alpha_2 \tag{17}$$

where α_1 and α_2 are assumed initial guesses which need to be determined. When $M = \gamma = A = R = \delta = 0$ and $Pr = 0.7$, comparisons of coefficient of skin friction for various rates of B with earlier published findings [31-33] are stated in Table 1 to assess the validity of the current numerical results. Also found is that an excellent link between the two variables has been established. Moreover, it is noted that a high degree of correlation is obtained.

Table 1. Values of $f''(0)$ for some values of B at $M = \gamma = A = R = \delta = 0$ and $Pr = 0.7$.

B	[31]	[32]	[33]	Present results
0.01	-0.9980	-0.9980	-0.99802	-0.998065
0.02	-0.9958	-	-0.99578	-0.995811
0.05	-0.9876	-	-0.98757	-0.987588
0.10	-0.9694	-0.9694	-0.96938	-0.969387
0.20	-0.9181	-0.9181	-0.91810	-0.918107
0.50	-0.6673	-0.6673	-0.66732	-0.667263
1.00	-	-	0.00000	0
2.00	-	2.0175	2.01750	2.0175027
3.00	-	4.7292	4.72928	4.729282
4.00	-	-	-	8.000429

4. RESULTS AND DISCUSSIONS

This section illustrates and discusses the effects of various relevant parameters such as velocity ratio parameter B, magnetic parameter M, permeability parameter Γ, heat generation/absorption coefficient A, thermal radiation R, Prandtl number Pr, and slip effect δ graphically on velocity and temperature profiles. In Figures 2–11, extensive numerical solutions are presented. The default values of the parameters considered as under, unless otherwise mentioned: $\gamma = 1, \Gamma = 0.1, \delta = 0.1, n = 0.2, A = B = M = 0.1$, and $Pr = 0.7$. In Tables 2 and 3, coefficient of skin friction and heat transfer rate for different thermal radiation and velocity slip parameter values are listed. The effects of radiation R parameter on the temperature and velocity profiles are illustrated in Figures 2-3, respectively. A rise in the radiation parameter results cause to rise in the temperature of the fluid being heated. Essentially, the radiative energy enhances the impact of temperature and conduction at respective place on the surface, as a result, a vast amount of radiation energy is created, which raises the temperature of the fluid. On the other hand, there is no noticeable change in the profile of velocity as a horizontal surface has been considered.

Table 2. Results of $f''(0)$ and $-\theta'(0)$ for different values of R with $\gamma = 1, \Gamma = 0.1, \delta = 0.1, n = 0.2, A = B = M = 0.1$ and $Pr = 0.7$.

R	$f''(0)$	$-\theta'(0)$
0	-1.338191965	0.945955902
0.3	-1.338191965	0.705378882
0.6	-1.338191965	0.574614931

Table 3. Results of $f''(0)$ and $-\theta'(0)$ for different values of δ when $= 1, \Gamma = 0.1, n = 0.2, A = B = M = 0.1$ and $Pr = 0.7$.

δ	$f''(0)$	$-\theta'(0)$
0	-1.616258037	0.729409419
0.1	-1.338191965	0.705378882
0.3	-1.006890697	0.673515832

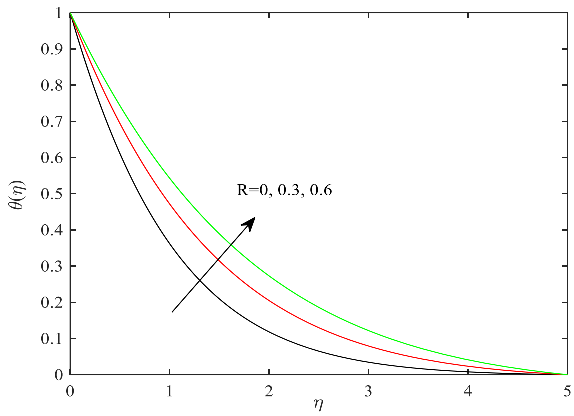

Figure 2. Temperature profile at different values of R with $\gamma = 1, \Gamma = 0.1, \delta = 0.1, n = 0.2, A = B = M = 0.1$

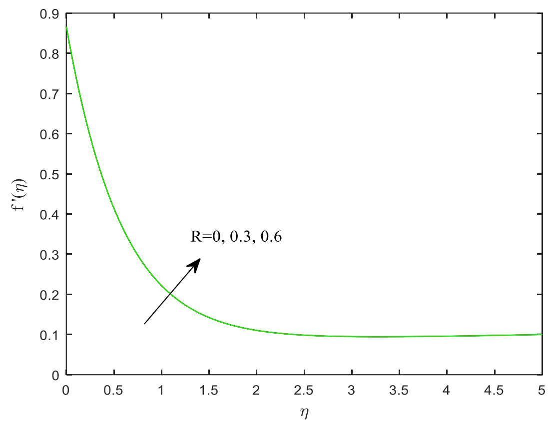

Figure 3. Velocity profile at different values of R with $\gamma = 1, \Gamma = 0.1, \delta = 0.1, n = 0.2, A = B = M = 0.1$ and $Pr = 0.7$.

Figures 4-5 illustrate the influence of the velocity slip parameter δ on the profiles of temperature and velocity in the presence of the other parameters. When slip effects grow, it has been observed that the temperature increases. However, by gradually increasing the values of the velocity slip parameter, it is possible to achieve a steady reduction in the velocity profiles. The effect of the "Prandtl number Pr on the temperature profile is depicted and seen in the Figure 6. The Prandtl number is defined as the ratio of the momentum diffusivity to the thermal diffusivity of a given system. The increase in the values of Pr leads in a decrease in the temperature profile, which in turn results in a decrease in the thickness of the thermal boundary layer. definitely, a lesser thermal diffusivity causes a rise in the Prandtl number, which in turn aids in the reduction of the thickness of the thermal boundary layer. Because of this increase in the Pr, the flow at the boundary is pulled down, resulting in a change in the thickness of the thermal boundary layer.

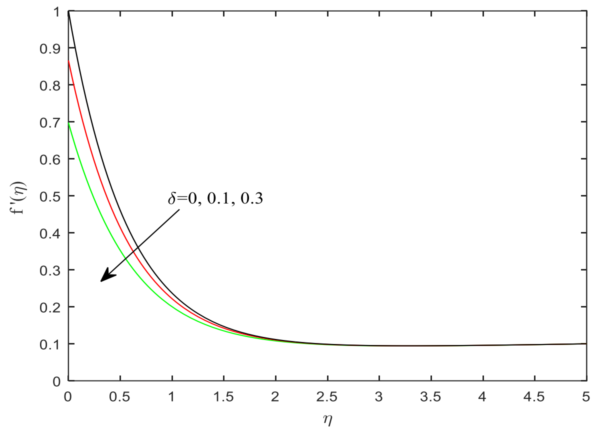

Figure 5. Velocity profile at different values of δ with $\gamma = 1, \Gamma = 0.1, n = 0.2, R = 0.3, A = B = M = 0.1$ and $Pr = 0.7$.

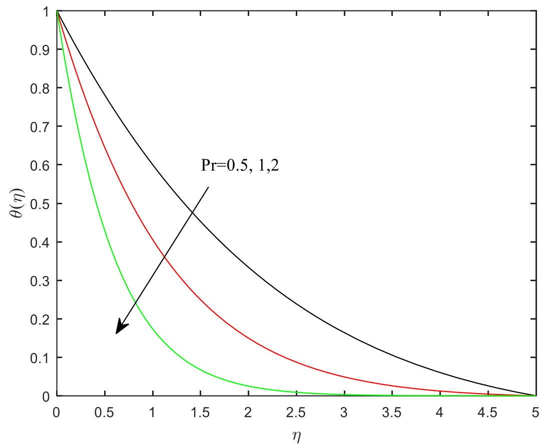

Figure 6. Temperature profile at different Pr with $\gamma = 1, \Gamma = 0.1, n = 0.2, A = 0.1, R = 0.3, B = 0.1$ and $M = 0.1$.

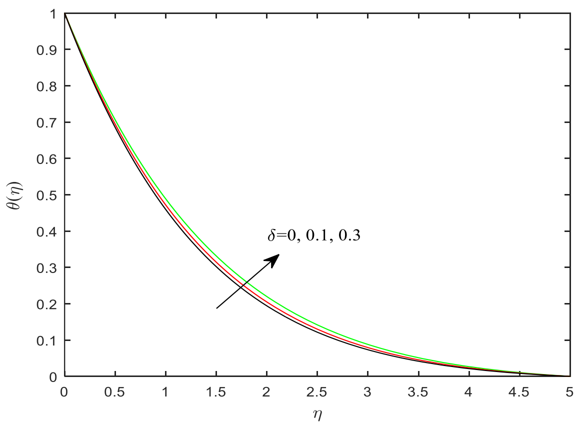

Figure 4. Temperature profile at different values of δ with $\gamma = 1, \Gamma = 0.1, n = 0.2, R = 0.3, A = B = M = 0.1$ and $Pr = 0.7$.

The effects of the suction parameter γ on the fluid velocity and temperature profiles are illuminated in Figures 7-8, respectively. From this point on, we can see that the profile reduces with an increase in the value of γ. The corresponding boundary layer thickness is also reduced, owing to the fact that the suction produces a reduction in the flow of the stream in a vertically descended manner. Also shown in Figure 8 is the relationship between the temperature and the suction/injection parameter γ. It is obvious that increasing γ decreases the temperature field. Because applying suction causes the number of fluid particles to be drawn into the wall, the temperature boundary layer drops.

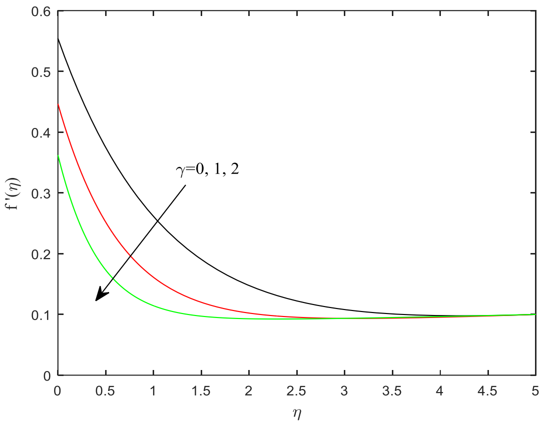

Figure 7. Velocity profile at different values of γ with $\Gamma = 0.1, n = 0.2, R = 0.3, A = B = M = 0.1$ and $Pr = 0.7$.

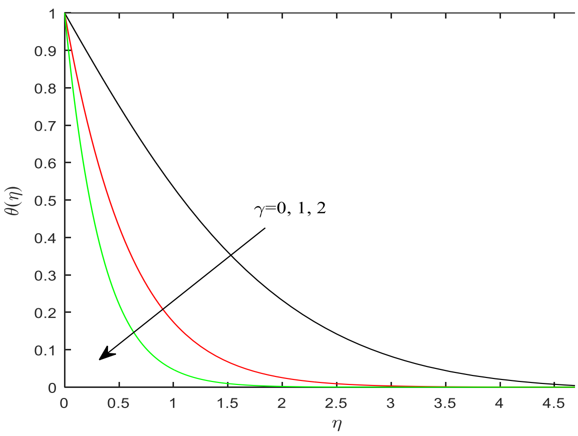

Figure 8. Temperature profile at different values of γ with $\Gamma = 0.1, n = 0.2, R = 0.3, A = B = M = 0.1$ and $Pr = 0.7$.

The values of $-\theta'(0)$ in the solution for the variation of Pr are shown in Figure 9, and it come to be positive for greater Prandtl number, indicating that heat moves from the heated surface to the ambient temperature of fluid. This fact also lends support to the previous findings of the current study, which show that temperature falls as the Prandtl number rises in significance. Furthermore, when the radiation parameter is expanded, the rate of heat transfer reduces; this fact demonstrates that heat flows from the ambient temperature in the direction of the heated surface. Slip effects, notwithstanding this, have the influence of slowing down the rate of heat transmission, as seen in Figure 10. The results of Figure 11 similarly corroborate those of Figure 10, where the heat transfer rate decreases as the thermal radiation parameter is raised to greater levels.

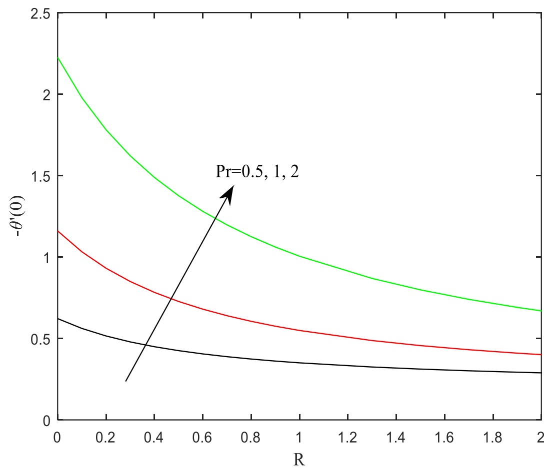

Figure 9. Temperature variation at different values of Pr with R at $\gamma = 1, \Gamma = 0.1, n = 0.2, A = 0.1, B = 0.1$ and $M = 0.1$.

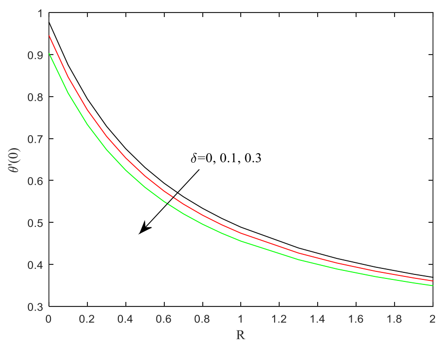

Figure 10. Temperature variation at different values of δ with R at $\gamma = 1, \Gamma = 0.1, n = 0.2, A = 0.1, B = 0.1, M = 0.1$ and Pr=0.7.

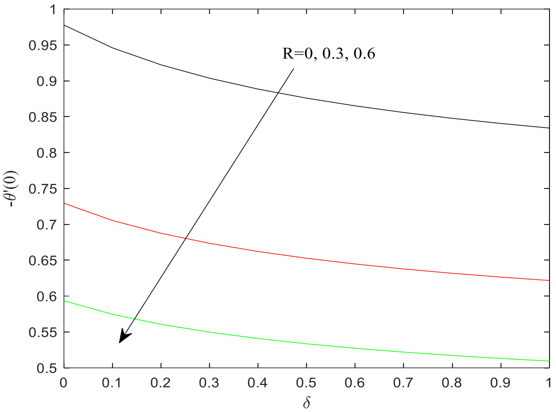

Figure 11. Temperature variation at different values of R with δ at $\gamma = 1, \Gamma = 0.1, n = 0.2, A = 0.1, B = 0.1, M = 0.1$and $Pr = 0.7$

DECLARATIONS

Funding: No funding was received for this study.

Conflicts of interest/Competing interests: The authors declare no any conflict of interest/competing interests.

Data availability: Not applicable

Code availability: Not applicable

Authors' contributions:

onceptualization, Ubaidullah Yashkun & Khairy Zaimi; Methodology, Ubaidullah Yashkun & Liaquat Ali Lund; Software, Ubaidullah Yashkun; Formal analysis, Ubaidullah Yashkun, Khairy Zaimi, Liaquat Ali Lund; Writing—original draft, Ubaidullah Yashkun & Liaquat Ali Lund; Supervision, Khairy Zaimi. All authors have read and agreed to the published version of the manuscript.

CONCLUSION

The aim of the current study was to offer a Three Stage Labatto Three a formula for addressing boundary value problems that included physical effects of various parameters. The equations of the electrically conducting incompressible fluid flow moving towards stagnation point through the stretched surface are approximated numerically in this study, and the results are presented in this paper. Flow modelling in porous media considers the impacts of heat source and sink, thermal radiation, velocity slip, magnetic field, and suction/injection parameters. Nonlinear ODEs are obtained from PDEs by the simulations of appropriate similarity transformations. Using the Three Stage Labatto Three A formula, the approximate solutions generated for the parameters: Nusselt number, skin friction coefficient, temperature profile, and velocity profile. The accuracy of the used method is validated by comparing current results to previously published literature. The following are the effects of relevant parameters:

a. When the suction parameter was set to greater levels, the conductivity of the skin friction increased.
b. The increasing value of the radiation parameter has ensured that the temperature profile along with the thickness of the thermal boundary layer have both raised.
c. The amount of suction S introduced into a steady fluid flow reduces the fluid flow velocity and temperature.
d. The increasing Prandtl number has guaranteed that profile of temperature and the thickness of the thermal layer have both decreased.
e. Because of a rise in the permeability parameter, the thickness of the boundary layer is increased.

REFERENCES

[1] K. Hiemenz, Die Grenzschicht an einem in den gleichformigen Flussigkeitsstrom eingetauchten geraden Kreiszylinder, Dinglers Polytech J 326 (1911), 321–324.

[2] B. C. Sakiadis, Boundary-layer behavior on continuous solid surfaces: I. Boundary-layer equations for two-dimensional and axisymmetric flow, AIChE Journal 7(1) (1961), 26-28.

[3] L. J. Crane, Flow past a stretching plate. Zeitschrift für angewandte Mathematik und Physik ZAMP, 21(4) (1970), 645-647.

[4] T. C. Chiam, Stagnation-point flow towards a stretching plate. Journal of the physical society of Japan, 63(6) (1994), 2443-2444.

[5] A. Ishak, R. Nazar, & I. Pop, Magnetohydrodynamics stagnation point flow towards a stretching vertical sheet. Magnetohydrodynamics, 42(1) (2006), 77-90.

[6] K. Sadeghy, H. Hajibeygi, & S. M. Taghavi, Stagnation-point flow of upper-convected Maxwell fluids. International Journal of Non-Linear Mechanics, 41(10) (2006), 1242-1247.

[7] H. A. Attia, Axisymmetric stagnation point flow towards a stretching surface in the presence of a uniform magnetic field with heat generation. 淡江理工學刊, 10(1) (2007), 11-16.

[8] S. E. Ghasemi, & M. Hatami, Solar radiation effects on MHD stagnation point flow and heat transfer of a nanofluid over a stretching sheet. Case Studies in Thermal Engineering, 25 (2021), 100898.

[9] N. Harada, & K. Tsunoda, Study of a disk MHD generator for nonequilibrium plasma generator (NPG) system. Energy conversion and management, 39(5-6) (1998), 493-503.

[10] J. S. Shang, Recent research in magneto-aerodynamics. Progress in Aerospace Sciences, 37(1) (2001), 1-20.

[11] M. Abricka, J. Krūminš, & Y. Gelfgat, Numerical simulation of MHD rotator action on hydrodynamics and heat transfer in single crystal growth processes. Journal of crystal growth, 180(3-4) (1997), 388-400.

[12] U. Yashkun, K. Zaimi, N. A. A. Bakar, Ishak, A., & Pop, I., MHD hybrid nanofluid flow over a permeable stretching/shrinking sheet with thermal radiation effect. International Journal of Numerical Methods for Heat & Fluid Flow, (2020).

[13] M. Darzi, M. Vatani, S. E. Ghasemi, & D. D. Ganji, Effect of thermal radiation on velocity and temperature fields of a thin liquid film over a stretching sheet in a porous medium. The European Physical Journal Plus, 130(5) (2015), 1-11.

[14] M. M. Nandeppanavar, M. S. Abel, & M. C. Kemparaju, Stagnation point flow, heat and mass transfer of MHD nanofluid due to porous stretching sheet through porous media with effect of thermal radiation. Journal of Nanofluids, 6(1) (2017), 38-47.

[15] M. S. Abel, & M. M. Nandeppanavar, Effects of thermal radiation and non-uniform heat source on MHD flow of viscoelastic fluid and heat transfer over a stretching sheet. International Journal of Applied Mechanics and Engineering, 12(4) (2007), 903-918.

[16] M. Mustafa, & J. A. Khan, Model for flow of Casson nanofluid past a non-linearly stretching sheet considering magnetic field effects. AIP advances, 5(7) (2015), 077148.

[17] S. Khalili, S. Dinarvand, R. Hosseini, H. Tamim, & I. Pop, Unsteady MHD flow and heat transfer near stagnation point over a stretching/shrinking sheet in porous medium filled with a nanofluid. Chinese physics B, 23(4) (2014), 048203.

[18] S. E. Ghasemi, M. Hatami, A. K. Sarokolaie, & D. D. Ganji, Study on blood flow containing nanoparticles through porous arteries in presence of magnetic field using analytical methods. Physica E: Low-dimensional Systems and Nanostructures, 70 (2015), 146-156.

[19] A. Asadi, I. M. Alarifi, & L. K. Foong, An experimental study on characterization, stability and dynamic viscosity of CuO-TiO2/water hybrid nanofluid. Journal of Molecular Liquids, 307 (2020), 112987.

[20] D. A. Nield, & A. Bejan, Convection in porous media (Vol. 3). New York: springer. (2006).

[21] B. Mohanty, S. R. Mishra, & H. B. Pattanayak, Numerical investigation on heat and mass transfer effect of micropolar fluid over a stretching sheet through porous media. Alexandria Engineering Journal, 54(2) (2015), 223-232.

[22] N. Sandeep, A. V. B. Reddy, & V. Sugunamma, Effect of radiation and chemical reaction on transient MHD free

convective flow over a vertical plate through porous media. Chemical and process engineering research, 2 (2012), 1-9.
[23] K. V. Prasad, M. S. Abel, & A. Joshi, Oscillatory motion of a viscoelastic fluid over a stretching sheet in porous media. Journal of Porous Media, (2000), 3(1).
[24] M. D. Shamshuddin, O, Anwar Bég, M. Sunder Ram, & A. Kadir, Finite element computation of multi-physical micropolar transport phenomena from an inclined moving plate in porous media. Indian Journal of Physics, 92(2) (2018), 215-230.
[25] I. Ullah, S. Shafie, & I. Khan, Effects of slip condition and Newtonian heating on MHD flow of Casson fluid over a nonlinearly stretching sheet saturated in a porous medium. Journal of King Saud University-Science, 29(2) (2017), 250-259.
[26] P. Agrawal, P. K. Dadheech, R. N. Jat, M. Bohra, K. S. Nisar, & I. Khan, Lie similarity analysis of MHD flow past a stretching surface embedded in porous medium along with imposed heat source/sink and variable viscosity. Journal of Materials Research and Technology, 9(5) (2020), 10045-10053.
[27] L. A. Lund, Z. Omar, & I. Khan, Darcy-Forchheimer porous medium effect on rotating hybrid nanofluid on a linear shrinking/stretching sheet. International Journal of Numerical Methods for Heat & Fluid Flow, (2021).
[28] S. Dero, L. A. Lund, R. N. Dara, M. Ayadi, S. U. Khan, & W. Chammam, Thermal efficiency and stability of copper-alumina nanoparticles with Darcy-Forchheimer effects. Waves in Random and Complex Media, (2022), 1-21.
[29] J. Raza, S. Dero, L. A. Lund, & Z. Omar, Duality and stability of MHD Darcy–Forchheimer porous medium flow of rotating nanofluid on a linear shrinking/stretching sheet: Buongiorno model. International Journal of Numerical Methods for Heat & Fluid Flow, (2021).
[30] S. G. Bejawada, Y. D. Reddy, W. Jamshed, K. S. Nisar, A. N. Alharbi, & R. Chouikh, Radiation effect on MHD Casson fluid flow over an inclined non-linear surface with chemical reaction in a Forchheimer porous medium. Alexandria Engineering Journal, 61(10) (2022), 8207-8220.
[31] T. M. Agbaje, S. Mondal, Z. G. Makukula, S. S. Motsa, & P. Sibanda, A new numerical approach to MHD stagnation point flow and heat transfer towards a stretching sheet. Ain Shams Engineering Journal, 9(2) (2018), 233-243.
[32] W. Ibrahim, B. Shankar, & M. M. Nandeppanavar, MHD stagnation point flow and heat transfer due to nanofluid towards a stretching sheet. International journal of heat and mass transfer, 56(1-2) (2013), 1-9.
[33] T. Hayat, T. Javed, & Z. Abbas, MHD flow of a micropolar fluid near a stagnation-point towards a non-linear stretching surface. Nonlinear Analysis: Real World Applications, 10(3) (2009), 1514-1526.
[34] S. Haq, & M. Sohaib, An Enhanced Wavelet Based Method for Numerical Solution of High Order Boundary Value Problems, J. mt. area res., 6 (2021), 63-76.

Received: 05 Jan. 2023. Revised/Accepted: 26 Feb. 2023.